

TOWARDS FOUNDATION MODELS FOR ZERO-SHOT TIME SERIES ANOMALY DETECTION: LEVERAGING SYNTHETIC DATA AND RELATIVE CONTEXT DISCREPANCY

Anonymous authors

Paper under double-blind review

ABSTRACT

Time series anomaly detection (TSAD) is a critical task, but developing models that generalize to unseen data in a zero-shot manner remains a major challenge. Prevailing foundation models for TSAD predominantly rely on reconstruction-based objectives, which suffer from a fundamental objective mismatch: they struggle to identify subtle anomalies while often misinterpreting complex normal patterns, leading to high rates of false negatives and positives. To overcome these limitations, we introduce `TimeRCD`, a novel foundation model for TSAD built upon a new pre-training paradigm: Relative Context Discrepancy (RCD). Instead of learning to reconstruct inputs, `TimeRCD` is explicitly trained to identify anomalies by detecting significant discrepancies between adjacent time windows. This relational approach, implemented with a standard Transformer architecture, enables the model to capture contextual shifts indicative of anomalies that reconstruction-based methods often miss. To facilitate this paradigm, we develop a large-scale, diverse synthetic corpus with token-level anomaly labels, providing the rich supervisory signal necessary for effective pre-training. Extensive experiments demonstrate that `TimeRCD` significantly outperforms existing general-purpose and anomaly-specific foundation models in zero-shot TSAD across diverse datasets. Our results validate the superiority of the RCD paradigm and establish a new, effective path toward building robust and generalizable foundation models for time series anomaly detection. The code is available in <https://anonymous.4open.science/r/TimeRCD-5BE1/>

1 INTRODUCTION

Time series anomaly detection (TSAD) is a crucial task in domains such as finance (Ahmed et al., 2016), healthcare (Kaji et al., 2019), industrial monitoring (Lan et al., 2025), and cloud operations (Ren et al., 2019). The accurate detection of rare and unexpected events is vital for ensuring system reliability and safety. Despite recent progress driven by deep learning, most existing approaches are trained in a dataset- and model-specific manner, which restricts their scalability and hampers generalization across diverse domains in a *zero-shot* way.

The success of foundation models in natural language processing and computer vision has motivated efforts to establish similar paradigms for TSAD. Existing approaches can be broadly categorized into two directions: (i) general-purpose time series foundation models designed for multiple tasks such as classification, forecasting, and anomaly detection (Gao et al., 2024; Goswami et al., 2024; Woo et al., 2024; Ekambaram et al., 2025; Xie et al., 2024), and (ii) anomaly-specific foundation models tailored explicitly for TSAD (Shentu et al., 2024). The more related work discussion is in Appx. B. Despite their differences, both types of mod-

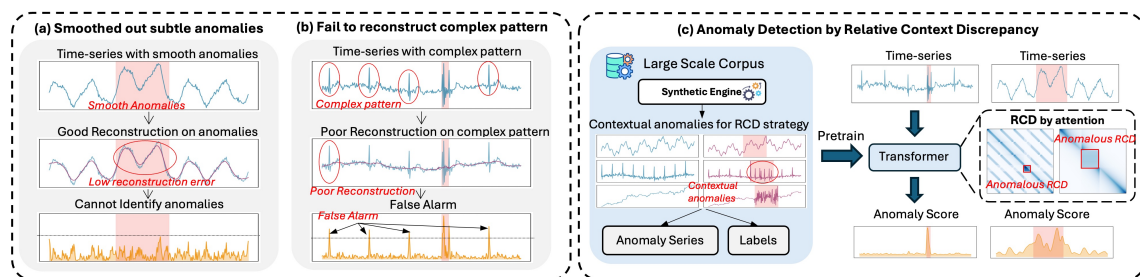


Figure 1: **Limitations of Reconstruction-based TSAD and Our Proposed TimeRCD.** (a) The model accurately reconstructs a smooth anomaly, resulting in a low error score and a missed detection (false negative). (b) The model fails to reconstruct a complex normal pattern unseen in the training dataset, leading to a high error score and a false alarm (false positive). (c) TimeRCD adopts RCD with a large-scale corpus and a standard Transformer-Encoder.

els predominantly rely on reconstruction-based objectives trained on real-world data, where anomalies are inferred indirectly from deviations between reconstructed and observed sequences.

While intuitive, reconstruction-based methods suffer from a fundamental **objective mismatch**: they are optimized to reconstruct normal patterns in a latent space where anomalous structure is assumed to be lost (Wong et al., 2022). This leads to critical limitations, as illustrated in Figure 1(a,b). First, subtle and contextual anomalies are often smoothed out and thus missed, resulting in low reconstruction error and false negatives (Wong et al., 2022; Wu et al.). Second, complex but normal sequences deviate from the “average” patterns learned during training, yielding high reconstruction errors and false alarms (Yahya et al., 2025). These weaknesses are further exacerbated in zero-shot settings, where unseen yet normal patterns make reconstruction-based scores particularly unreliable. Our experiments confirm this gap: reconstruction-based foundation models achieve only 15.4% Standard-F1 on contextual anomalies, compared to 82.7% for our RCD approach (Section 3.3.)

Additional fragilities arise from the limitations of real-world training data. First, labeled anomalies are inherently **scarce**, providing the model with few examples to learn abnormal behavior. Second, training data often lacks **diversity**, covering only a subset of real-world patterns. In zero-shot scenarios, these data limitations leave models unexposed to many unseen normal and abnormal sequences, hindering their ability to generalize and detect novel anomalies. To mitigate these issues, some approaches have focused on data augmentation, where artificial anomalies are injected into real-world time series to enrich the training set (Shentu et al., 2024; Darban et al., 2025; Cai et al., 2024). However, these methods are still fundamentally dependent on the availability and diversity of the underlying real data they seek to enhance. Consequently, in zero-shot and cross-domain scenarios, these data limitations leave models unexposed to many unseen normal and abnormal sequences, hindering their ability to generalize and detect novel anomalies.

To address these limitations, we introduce `TimeRCD`, a novel foundation model for TSAD built on a new pre-training paradigm, as illustrated in Figure 1(c). Our approach abandons indirect reconstruction-based objectives in favor of explicitly learning to detect anomalies through **Relative Context Discrepancy** (RCD). The fundamental insight behind RCD is that many anomalies, particularly subtle or contextual ones, are best identified not in isolation but as a significant discrepancy between the patterns of adjacent time windows. By capturing these relational differences, our model can detect shifts that single-window analysis would otherwise miss.

For our pre-training process, we employ a standard Transformer backbone without any architectural modifications. We treat each time window of a time series as an input token, which allows the self-attention

mechanism to naturally compute the inter-token relationships. As shown in Figure 1(c), the model’s attention weights learn to capture the discrepancy between contexts, effectively identifying anomalous RCD. An anomaly scoring head then uses these learned discriminative features to produce a final score. To teach the model this explicit detection strategy, we provide it with a rich, supervised signal by first leveraging a synthetic engine. This engine generates a large-scale, diverse, and fully-labeled corpus of time series data that is specifically designed to contain a wide variety of contextual anomalies, enabling the model to learn the RCD task from the ground up. Our main contribution are threefold:

- **The Relative Context Discrepancy (RCD) strategy and the TimeRCD model** We introduce a novel pre-training paradigm for time series anomaly detection that moves beyond reconstruction by explicitly learning to identify anomalies through RCD. This strategy is instantiated in our foundation model, TimeRCD, which uses a standard Transformer to capture relational differences between time windows. This design achieves strong zero-shot generalization through a simple yet powerful architecture.
- **A large-scale, fully-labeled synthetic corpus for foundation models** To enable the RCD pre-training paradigm and its rigorous evaluation, we construct a comprehensive synthetic corpus. It provides token-level annotations for a diverse spectrum of anomalies, including point, contextual, and collective types with cross-variate propagation, offering the essential supervision for building and evaluating zero-shot TSAD models on this corpus.
- **Extensive empirical evaluation** Experiments on diverse corpora demonstrate consistent gains over existing reconstruction-based and general-purpose time-series foundation models. Ablation studies confirm the contributions of both the synthetic corpus and the RCD framework to zero-shot performance.

2 METHODOLOGY: THE TIMERCD FRAMEWORK

In this section, we first formally define the zero-shot time series anomaly detection task. We then present the RCD strategy and the foundation model architecture (Section 2.1), which employs an encoder-only Transformer. Finally, we introduce our synthetic data generation engine (Section 2.2), producing a rich, diverse, and precisely annotated training corpus.

Problem Definition For the zero-shot time series anomaly detection problem, we observe a multivariate d -channel time series $\mathbf{X} = (\mathbf{x}_1, \dots, \mathbf{x}_n)$ with $\mathbf{x}_t \in \mathbb{R}^d$ for each time step $t \in [n] := \{1, 2, \dots, n\}$. The objective is to produce a binary annotation sequence $\hat{\mathbf{y}} = (\hat{y}_1, \dots, \hat{y}_n) \in \{0, 1\}^n$ such that $\hat{y}_t = 1$ if and only if time t is anomalous. In the zero-shot setting, the model must detect anomalies on unseen target sequences without any additional training or fine-tuning, distinguishing normal from anomalous behavior.

2.1 RCD STRATEGY AND FOUNDATION MODEL ARCHITECTURE

Relative Context Discrepancy We introduce RCD to redefine zero-shot anomaly detection in time series. Rather than learning discriminative mappings from individual samples to labels, RCD formulates detection as comparing a set of time windows to extract discriminative relational patterns. This approach derives anomaly scores from relational comparisons, enabling the model to detect subtle and comparative anomalies in unseen sequences under the zero-shot setting. [Detailed mathematical formulation of RCD is provided in Appx. C.](#)

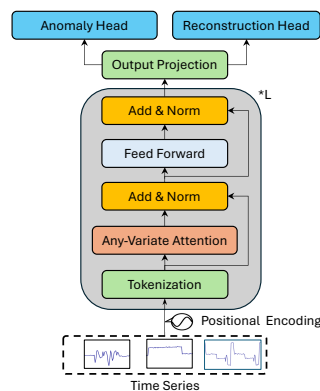


Figure 2: TimeRCD Architecture

141 Concretely, when each time window is treated as an input token, the Transformer’s self-attention effectively implements RCD: attention weights naturally capture relational discrepancies among windows within
 142 the sequence context. This demonstrates that RCD-based anomaly detection can be directly realized using
 143 standard Transformer blocks. Building on this, we propose a novel foundation model, TimeRCD, illustrated in Fig. 2, which adopts an encoder-only Transformer (Vaswani et al., 2017) with input tokenization,
 144 Transformer blocks, and output projection. Crucially, our approach leverages the existing Transformer architecture directly, requiring no structural modifications, which underscores both its simplicity and broad
 145 applicability.

149 **Variate-Window Tokenization** We adopt the common practice (Nie et al., 2022) and treat a window of
 150 continuous observations as an input token. Since multivariate anomaly detection is a critical task (Zaman-
 151 zadeh Darban et al., 2024), we build on the design introduced by Moirai (Woo et al., 2024), which flattens
 152 multivariate time series so that all variates are represented within a single sequence. This design allows the
 153 subsequent Transformer blocks to capture both intra-variate dependencies and inter-variate dependencies.
 154 Specifically, given a normalized multivariate time series $\tilde{\mathbf{X}} \in \mathbb{R}^{n \times d}$, we partition it into $\lceil n/W \rceil \times d$ non-
 155 overlapping windows, where W denotes the window length. The resulting windows are then flattened
 156 and linearly projected into input token embeddings $\mathbf{H}_{inp} \in \mathbb{R}^{\lceil n/W \rceil d \times D_v}$.

158 **Transformer Blocks** We stack L transformer blocks, each consisting of layer normalization, feed-forward
 159 network, and self-attention modules. The architecture imposes no special requirements on the Transformer
 160 block itself; however, the self-attention mechanism is repurposed to compute the RCD. Each token attends
 161 to other tokens, capturing inter-tokens differences that serve as contrastive features for subsequent anomaly
 162 score computation. Specifically, we leverage the any-variate attention (Woo et al., 2024) and formulate the
 163 output token embeddings as $\mathbf{H}_{out} \in \mathbb{R}^{\lceil n/W \rceil d \times D_v}$.

165 **Output Projection and Anomaly/Reconstruction Head** To derive anomaly scores at the original tempo-
 166 ral resolution, the output token embeddings \mathbf{H}_{out} from the Transformer blocks are projected back into the
 167 observation space. Concretely, we define two heads during training: $\mathbf{X}_{rec} = \mathbf{H}_{out} \mathbf{W}_s \mathbf{W}_{rec}$ and
 168 $\mathbf{X}_{ano} = \mathbf{H}_{out} \mathbf{W}_s \mathbf{W}_{ano}$, where $\mathbf{W}_s \in \mathbf{R}^{D_v \times D_v}$ is the shared embedding projection, $\mathbf{W}_{rec} \in \mathbf{R}^{D_v \times W}$
 169 and $\mathbf{W}_{ano} \in \mathbf{R}^{D_v \times W}$ are the reconstruction and anomaly projection, respectively. The reconstruction head
 170 predicts masked portions of the input series. **To foster robust contextual learning, we employ a patched
 171 masking strategy where continuous segments of the input time series are masked (with a 15% ratio), as
 172 opposed to random point masking. This design prevents information leakage from adjacent timestamps and
 173 compels the model to reconstruct missing patterns by aggregating global context. Concurrently, the anomaly
 174 head outputs window-level anomaly scores. We optimize the model using a joint loss function:**

$$175 \mathcal{L} = \|\mathbf{M} \odot (\mathbf{X}_{rec} - \mathbf{X})\|_2^2 + \text{BCE}(\sigma(\mathbf{X}_{ano}), \mathbf{y}),$$

176 where \mathbf{M} is the binary mask, \mathbf{y} denotes ground-truth labels, and σ is the sigmoid function. During inference,
 177 no masking is applied. The model processes the full, uncorrupted time series, and the Reconstruction Head
 178 is discarded. **Only the Anomaly Head is used to compute anomaly scores.** Although the reconstruction
 179 head is discarded at inference, it acts as a crucial auxiliary task during training, encouraging the transformer
 180 blocks to learn rich, stable embeddings beyond pairwise relational discrepancies. This effect is empirically
 181 validated in Appx. F.6.

182 We design a synthetic engine to generate multivariate time series with rich, controllable contextual structures,
 183 creating a TSAD benchmark that encourages models to recognize anomalies relative to context. The pipeline
 184 proceeds in three hierarchical stages: first, defining univariate contextual patterns (Stage 1); next, integrating
 185 them into a multivariate system with causal dependencies (Stage 2); and finally, injecting context-aware
 186 anomalies that depend on the system’s structure (Stage 3). A summary is shown in Fig. 3, with full details
 187 in Appx. D.

2.2 SYNTHETIC DATA GENERATION

Stage 1: Context-Template Generation For each channel, we generate normal context data from an additive template: $x_{\text{base}}(t) = T(t) + S(t) + \varepsilon(t), t = 0, 1, \dots, n - 1$. The trend blends deterministic and stochastic components, i.e., $T(t) = (1 - \rho_T)T_{\text{det}}(t) + \rho_T T_{\text{stoc}}(t)$. Seasonality is a mixture of periodic atoms, i.e., $S(t) = \sum_{k=1}^K A_k w_k(2\pi f_k t + \varphi_k; \theta_k)$, where w_k spans sinusoid, square/triangle waves, and wavelet atoms with amplitudes A_k , frequencies f_k , phases φ_k , and shape parameters θ_k . Noise is zero-mean with optional piecewise volatility, e.g., $\varepsilon(t) \sim \mathcal{N}(0, \sigma^2(t))$ and $\sigma(t)$ allowing bursty segments. The full description for constructing trend and seasonality is in Appx. D.2 and D.3.

Stage 2: Joint-Context Fusion To simulate realistic inter-channel dependencies, we fuse per-channel contexts into a coherent multivariate system via a causal graphical model. We first sample a DAG $G = (V, E)$ over N channels (nodes) and define a latent causal process z_i for each node. Discretizing first-order ODE dynamics by Euler ($\Delta t = 1$) gives an ARX system: $z_i[t] = a_i z_i[t - 1] + \sum_{j \in P(i)} b_{ij} x_j[t - \ell_{ij}] + c_i, |a_i| \leq 0.8$, with parent set $P(i)$, lags ℓ_{ij} , gains b_{ij} , and bias c_i . The observed signal mixes baseline and causal channels $x_i[t] = (1 - \alpha_i) x_{\text{base},i}(t) + \alpha_i z_i[t], \alpha_i \in [0, 1]$.

Stage 3: Causal-contextual Anomaly Injection

Most existing works inject anomalies via simple pointwise corruption or handcrafted signal perturbations—procedures that ignore both temporal context and cross-variate dependencies. We term this class **exogenous injections**, where a multivariate normal system is first generated and then a window in one channel is overwritten, i.e., $x'_{\text{anom},i}[t] = x_i[t] + \Delta(t)$ for $t \in [t_s, t_e]$. Beyond this, we introduce a novel **endogenous injection mechanism** that intervenes prior to causal mixing. Specifically, we perturb the baseline signal $x_{\text{base},i}$ of a parent node, i.e. $x'_{\text{base},i}(t) = x_{\text{base},i}(t) + \Delta(t)$ for $t \in [t_s, t_e]$, allowing abnormal effects to propagate to downstream nodes $x'_{\text{anom},j}[t]$ organically via the ARX dynamics. This process emulates internal system failures and yields multivariate anomalies with coherent temporal and structural footprints. We design more than 20 types of anomalies for $\Delta(t)$ and also consider a type of contextual anomalies which modifies the periodic structure, e.g., replace $S(t)$ with $S'(t)$ to realize frequency or phase shifts within $[t_s, t_e]$. The full taxonomy and parameterizations are detailed in Appx. D.4.

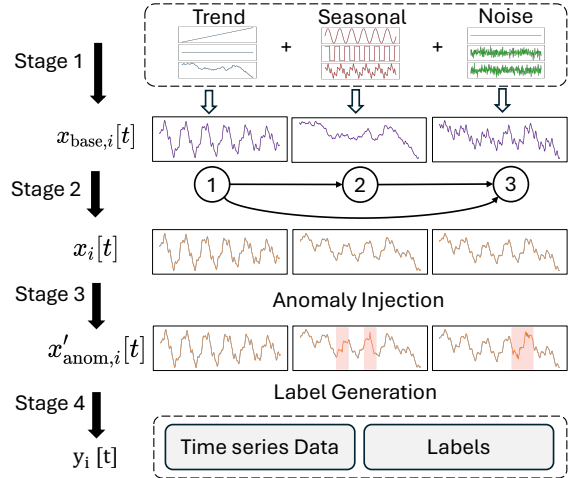


Figure 3: Synthetic data generation procedure.

Stage 4: Labels and Masks We generate token-level binary labels. For exogenous injections, positive labels correspond to the intervention window. For endogenous injections, we label the root-cause window and extend it to descendant channels based on their causal lags, as implied by the DAG and ARX lags $\{\ell_{ij}\}$. While our generation process tracks channel-specific anomalies (root-cause vs. propagated effects), for this work, we aggregate these into temporal localization labels (marking when an anomaly occurs across any channel). This aligns with standard zero-shot anomaly detection benchmarks, which typically provide timestep-level but not channel-level ground truth. Sequence lengths, DAG sparsity, ARX coefficients, and

235 signal regimes (trend, seasonality, noise) are sampled from configurable priors (Appx. D.1), generating rich,
236 interpretable dynamics designed for zero-shot learning.

237
238 **Relative Context Discrepancy** This layered generation process is designed to compel a model to learn
239 RCD. Rather than identifying anomalies via absolute thresholds or isolated patterns, a model must deter-
240 mine whether a data point is abnormal relative to its context. This context is multifaceted, including a
241 variable’s own temporal dynamics (e.g., trend, seasonality), its causal relationships with other variables, and
242 the characteristics of the anomaly itself. Our **endogenous anomaly** injection mechanism exemplifies this
243 challenge: a deviation in a downstream “child” variable may be a propagated effect of an upstream “parent”
244 failure. Correctly identifying only the root-cause anomaly requires the model to evaluate multiple variables
245 in light of their causal dependencies. This encourages reasoning beyond simple pattern recognition toward
246 a relational, system-level understanding—the essence of assessing relative discrepancy.

247 248 3 EXPERIMENTS

249
250 To validate the effectiveness of TimeRCD, we design a comprehensive evaluation to answer three research
251 questions: **RQ1**: How well does TimeRCD perform in strict zero-shot anomaly detection compared with
252 existing time-series foundation models and with full-shot, dataset-specific baselines? **RQ2**: How does the
253 RCD-based strategy exploit long contextual windows, and what is its impact on detecting contextual anom-
254 alies and on window-size sensitivity? **RQ3**: How do our synthetic generator and injection design affect
255 performance, and how does accuracy scale with pre-training data size?

256 257 3.1 EXPERIMENTAL SETTINGS

258 **Datasets** Our evaluation is conducted on a comprehensive suite of 16 public time-series anomaly detection
259 datasets, covering a wide range of real-world and synthetic scenarios. Details about the benchmark datasets
260 can be found in the Appx. E.1.

261
262 **Baselines** We benchmark TimeRCD against methods from two primary settings: (1) **Zero-shot models**,
263 which include our approach and other foundation models (DADA[†] (Shentu et al., 2024), TS-Pulse (Ekam-
264 baram et al., 2025), MOMENT[†] (Goswami et al., 2024), TimesFM (Das et al., 2024), Chronos (Ansari
265 et al., 2024), Time MOE (Shi et al., 2024)). (2) **Full-shot models**, which are fitted on a per-dataset basis.
266 This category includes deep learning methods (TranAD (Tuli et al., 2022), USAD (Audibert et al., 2020),
267 OmniAnomaly (Su et al., 2019), Sub-PCA (Liu & Paparrizos, 2024), DCdetector (Yang et al., 2023), TF-
268 MAE (Fang et al., 2024)) and classical statistical algorithms (LOF (Breunig et al., 2000), IForest (Liu et al.,
269 2008)). Note that models marked with (†) were excluded where necessary due to potential data leakage un-
270 der zero-shot setting (Appx. E.3). Additionally details about all of the baselines can be found at the Appx.
271 E.2.

272 **Evaluation Protocol** We evaluate model performance using four standard metrics: Affiliation-F1, F1-T,
273 Standard-F1, and VUS-PR. We deliberately avoid using the Point-Adjusted F1 score, as recent work has
274 demonstrated that Point Adjustment (PA) can lead to inflated and misleading performance evaluations (Huet
275 et al., 2022; Wang et al., 2023a). More details about the metrics are shown in the Appx. E.4.

276 277 3.2 MAIN RESULTS: TSAD ACCURACY (RQ1)

278
279 Our evaluation includes two comparisons: a direct **zero-shot** test against foundation models, and a **full-shot**
280 test against baselines trained on target data. We stress that **TimeRCD** is strictly zero-shot in all settings,
281 testing true out-of-the-box performance. Results are shown in Table 1. In zero-shot comparisons, TimeRCD

achieves clear SOTA: on 64 evaluation cases (16 datasets \times 4 metrics) it ranks first in **41** and second in **6**. Even against full-shot baselines with access to target data, TimeRCD is highly competitive, ranking first in **32** and second in **3**. This strong showing highlights the power and generalizability of our pre-training framework.

Table 1: Performance of **TimeRCD** against zero-shot and full-shot baselines. TimeRCD operates in a strictly zero-shot capacity in all comparisons. Best result is in **red**, second-best is in **blue**. Asterisk (*) results are excluded from ranking due to data leaking.

Metric	Model	Univariate Datasets										Multivariate Datasets				Total 1st	Total 2nd		
		IOPS	MGAB	NAB	NEK	Power	SED	Stock	TODS	UCR	WSD	YAHOO	MSL	PSM	SMAP			SMD	SWaT
Zero-Shot Models																			
Affiliation-F	TimeRCD	83.28	70.69	82.48	79.73	85.51	96.87	71.84	86.37	84.63	90.33	96.65	81.16	81.61	87.73	92.58	71.55	09	02
	DADA ¹	89.37*	67.66*	86.56	95.40	69.79	65.18	98.77	76.89	72.21	93.92	92.20*	76.57	81.27	76.92	83.74	76.18	03	06
	TS-Pulse	68.76	67.33	70.80	73.05	69.94	67.44	67.93	67.90	67.70	68.22	70.05	70.14	70.28	69.21	68.21	71.18	00	00
	MOMENT [†]	87.54*	66.76*	90.45*	92.26	75.97	59.13	45.26	59.76	75.77	95.39	79.99*	74.55*	65.79	77.42*	74.00*	70.17	01	02
	Chronos	81.88	66.95	79.73	90.49	69.88	67.14	97.53	89.08	70.03	78.97	91.28	20.35	71.24	45.44	62.85	44.37	00	02
FI-T	TimeRCD	83.28	70.69	82.48	79.73	85.51	96.87	71.84	86.37	84.63	90.33	96.65	81.16	81.61	87.73	92.58	71.55	09	02
	DADA ¹	42.50*	0.91*	37.24	47.08	19.80	9.56	95.49	35.18	7.22	48.46	79.52*	34.58	31.84	30.42	40.80	35.13	03	05
	TS-Pulse	4.10	0.81	34.61	27.07	19.90	9.71	15.98	13.45	5.12	4.57	5.50	23.57	25.39	12.34	9.15	28.58	00	00
	MOMENT [†]	33.15*	0.80*	52.27*	63.66	19.91	9.54	18.04	17.47	13.02	41.98	11.69*	25.97*	27.77	17.93*	28.68*	28.76	01	03
	TimesFM	48.95	0.93	36.74	36.63	19.80	9.58	88.94	51.13	10.78	41.38	83.46	7.83	25.42	11.64	18.65	21.39	01	01
Standard-FI	TimeRCD	24.22	1.62	27.70	33.05	28.59	69.88	32.61	67.02	28.13	31.96	87.02	30.66	26.00	30.48	44.89	28.73	11	01
	DADA ¹	32.76*	0.80*	26.91	48.24	15.99	2.69	95.59	28.18	3.36	45.06	79.30*	22.13	24.07	26.75	34.98	34.78	03	05
	TS-Pulse	3.54	0.73	21.61	23.96	18.27	8.84	15.46	12.45	2.05	2.17	4.00	12.56	22.31	7.44	8.00	23.84	00	01
	MOMENT [†]	30.69*	0.67*	44.75*	63.85	16.39	3.36	19.38	14.64	9.00	41.42	10.54*	14.43*	23.83	12.92*	29.78*	21.30	01	02
	TimesFM	34.28	0.83	26.46	38.15	16.73	2.96	89.13	40.08	7.86	38.50	84.44	5.75	22.18	10.46	18.65	22.84	01	01
VUS-PR	TimeRCD	20.23	1.05	24.32	27.88	21.25	80.75	77.28	93.46	23.09	21.77	84.41	20.45	18.69	22.68	37.03	17.58	10	02
	DADA ¹	24.97*	0.57*	24.73	46.85	10.61	6.42	99.51	64.83	2.94	33.42	70.74*	12.74	17.17	20.02	25.98	21.13	03	06
	TS-Pulse	4.64	0.56	16.40	19.39	11.72	9.11	70.95	45.86	1.20	1.83	9.93	7.41	14.48	3.99	4.56	15.67	00	01
	MOMENT [†]	37.35*	0.56*	45.38*	67.74	10.50	4.31	76.97	56.45	6.17	55.26	30.81*	9.32*	16.48	8.97*	15.96*	14.90	02	00
	Chronos	19.56	0.58	24.01	35.02	10.44	6.13	98.39	72.89	6.03	21.57	86.78	11.84	14.76	16.95	13.02	19.43	01	04
TimeRCD Grand Total (Zero-Shot)																			
Full-Shot Models																			
Affiliation-F	TimeRCD	83.28	70.69	82.48	79.73	85.51	96.87	71.84	86.37	84.63	90.33	96.65	81.16	81.61	87.73	92.58	71.55	10	01
	TranAD	83.19	67.28	90.28	85.02	71.56	61.03	57.94	52.76	73.31	84.34	76.08	79.91	73.83	87.39	92.09	75.37	00	04
	USAD	71.08	67.81	91.54	71.13	76.48	55.60	35.92	47.90	76.00	65.10	53.05	81.86	57.86	87.25	85.09	75.06	00	01
	OmniAnomaly	80.32	67.35	92.35	86.30	78.16	61.26	75.24	50.73	73.53	78.02	71.31	83.15	58.17	91.38	85.82	73.39	03	02
	LOF	81.06	68.44	75.75	84.74	66.76	63.85	69.74	60.58	73.53	81.29	75.63	84.35	61.98	63.32	64.13	56.34	01	00
FI-T	TimeRCD	83.28	70.69	82.48	79.73	85.51	96.87	71.84	86.37	84.63	90.33	96.65	81.16	81.61	87.73	92.58	71.55	09	02
	TranAD	52.81	68.82	39.84	71.15	0.00	70.09	0.06	44.17	50.56	41.24	33.30	63.36	63.78	59.96	69.71	0.00	00	01
	Sub-PCA	75.39	66.90	89.29	97.10	71.37	67.14	70.63	72.75	76.66	76.45	75.85	84.25	71.49	90.08	85.80	76.29	02	04
	DCdetector	71.83	67.91	72.21	62.31	69.75	72.20	55.79	57.81	70.18	72.79	67.77	67.74	67.32	67.10	69.55	71.07	00	01
	TFMAE	78.25	67.50	75.99	76.91	70.30	68.17	56.39	62.83	70.60	80.25	76.87	75.70	70.07	75.36	70.85	75.72	00	02
Standard-FI	TimeRCD	24.22	1.62	27.70	33.05	28.59	69.88	32.61	67.02	28.13	31.96	87.02	30.66	26.00	30.48	44.89	28.73	06	01
	TranAD	34.85	1.46	27.33	60.36	22.36	2.63	16.23	11.94	4.40	20.23	5.70	29.60	25.63	25.11	43.99	61.86	00	02
	USAD	30.66	3.89	56.15	62.91	28.24	3.41	17.99	23.87	10.74	13.20	7.21	38.71	28.41	38.66	53.06	62.82	03	02
	OmniAnomaly	47.05	1.44	28.81	74.03	23.50	0.43	38.59	12.65	5.11	29.57	21.40	39.10	30.43	40.50	57.06	55.93	04	04
	LOF	30.28	1.05	24.04	56.92	12.18	4.11	66.20	25.77	4.70	22.62	48.95	30.65	18.80	18.70	8.41	29.08	01	02
VUS-PR	TimeRCD	20.23	1.05	24.32	27.88	21.25	80.75	77.28	93.46	23.09	21.77	84.41	20.45	18.69	22.68	37.03	17.58	08	00
	TranAD	21.61	0.64	24.82	61.63	13.04	5.75	78.08	47.33	2.25	12.20	25.78	14.78	16.49	13.37	28.34	47.37	01	00
	USAD	16.58	0.75	55.03	58.53	18.68	4.37	74.53	56.36	8.85	10.00	14.15	29.95	17.59	26.37	34.53	44.73	01	04
	OmniAnomaly	25.35	0.64	27.17	74.51	14.32	6.20	91.29	45.55	2.40	16.37	29.26	31.57	18.58	28.07	37.44	42.97	04	03
	LOF	19.43	0.57	21.18	58.52	9.31	6.81	83.07	49.14	2.39	12.85	41.37	24.67	13.58	10.59	4.40	14.50	00	02
TimeRCD Grand Total (Full-Shot)																			

3.3 RCD STRATEGY EFFICIENCY (RQ2)

Qualitative Analysis of Contextual Understanding A key architectural feature of TimeRCD is its ability to process long context windows, allowing it to learn complex temporal dependencies. Many existing

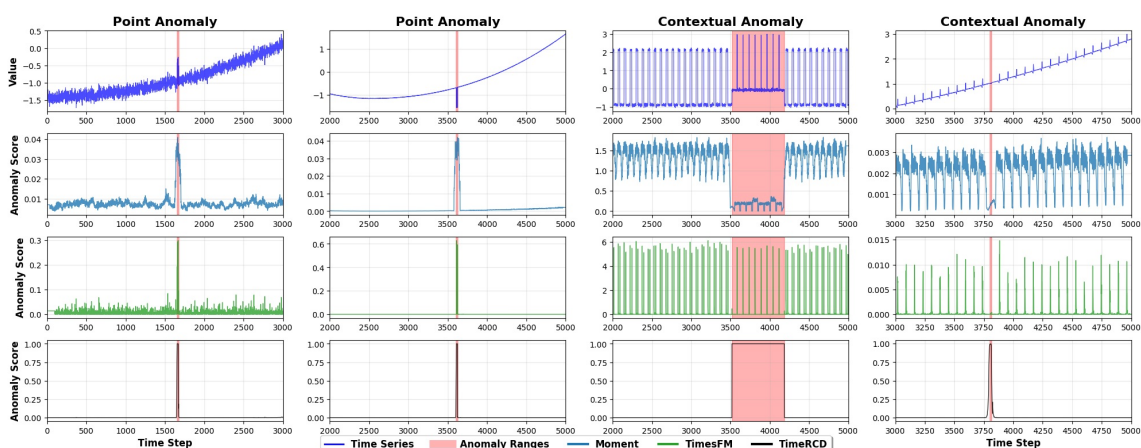


Figure 4: Qualitative comparison of anomaly scores.

zero-shot methods, particularly those based on reconstruction with small look-up windows, are effective at detecting abrupt **point anomalies**—short-term deviations from an immediate pattern (two left charts in Fig. 4). However, these models often fail on subtle **contextual**, where the anomalous behavior is a deviation from a long-term pattern (two right charts in Fig. 4). Their limited context prevents them from distinguishing normal long-term variations from true anomalous segments. In contrast, as our qualitative results in Fig. 4 show, TimeRCD’s ability to view the entire series allows it to learn the complex relationships between distant points.

Quantitative Analysis of Contextual Understanding We create specialized, unseen datasets containing either purely point or contextual anomalies, ensuring a fair zero-shot evaluation (details in Appx. F.2). The results are in Fig. 5. While TimeRCD’s performance on point anomalies is highly competitive with other top zero-shot models, it is substantially superior on contextual anomalies. On this task, our model achieves a Standard-F1 of 0.827, whereas all other models suffer a significant performance collapse. This performance disparity provides strong evidence that TimeRCD’s ability to leverage long-range context is a key capability, allowing it to detect complex deviations that are challenging for methods with a more limited contextual view.

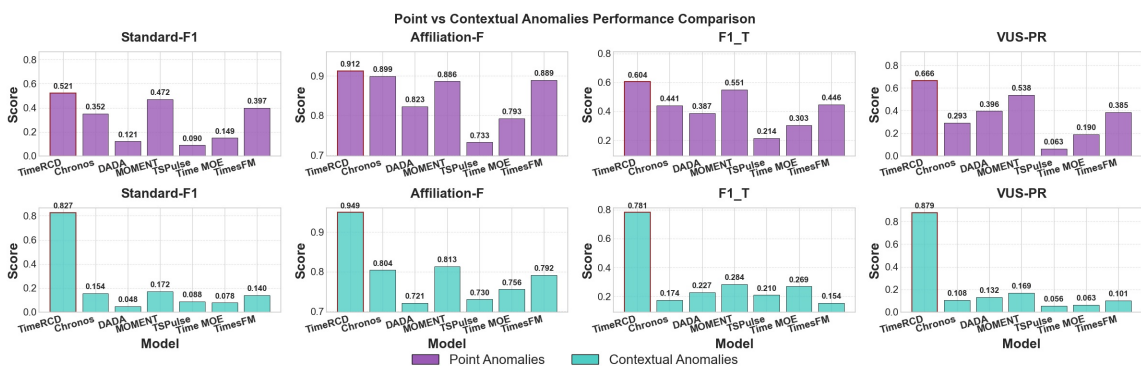


Figure 5: Comparison on specially-created datasets containing either point or contextual anomalies.

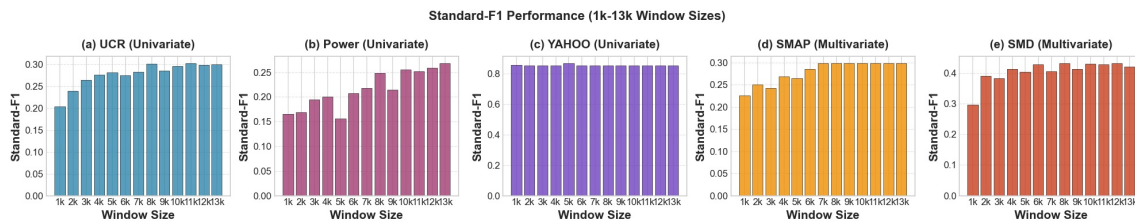


Figure 6: Performance on univariate (top) and multivariate (bottom) datasets as a function of the input window size, varied from 1k to 13k.

Impact of Context Window Size TimeRCD’s ability to process variable context lengths is a core architectural feature. To analyze its impact, we evaluate performance with input window sizes from 1k to 13k. As shown in Fig. 6, the results confirm that the optimal context length is task-dependent. For datasets with long-term patterns like **UCR**, **Power**, **SMAP**, and **SMD** Fig. 6 (a, b, d, e), performance generally improves with a larger window, as this allows the model to establish a more robust baseline of “normal” behavior. Conversely, on inherently short series like **YAHOO** Fig. 6(c), performance remains flat, as the series length itself becomes the effective context limit. A detailed breakdown for all datasets is available in Appx. F.3.

3.4 SYNTHETIC DATA EFFICIENCY (RQ3)

Ablation Study on Pre-training Data To validate our data generation framework, we train on the same TimeRCD (architecture, hyperparameters, epochs) on three 350M-point datasets, each with 350M points to match the real-world data scale: (1) our synthetic data with *in-context* anomaly injection, (2) the same synthetic series but with DADA-injected anomalies (Shentu et al., 2024), and (3) real-world data (Godahewa et al.) augmented with DADA. Table 2 shows weighted averages over 9 univariate benchmarks (full results in Appx. F.4). Models trained on augmented real data performed far worse, confirming the necessity of a high-quality synthetic curriculum. Comparing the two synthetic variants reveals a key trade-off: though using DADA-injection achieves similar Affiliation-F and slightly higher VUS-PR, it causes sharp drops in finer-grained metrics (F1-T \downarrow 6.4%, Standard-F1 \downarrow 6.1%). This indicates our in-context injection generates more challenging and robust training signals.

Table 2: Weighted average performance across 9 univariate benchmarks.

Pre-Training Dataset	Affiliation-F	F1-T	Standard-F1	VUS-PR
Our Synthetic Data	0.878	0.569	0.523	0.478
Our Synthetic + DADA Injection	0.878	0.505	0.462	0.487
Real-world Data + DADA Injection	0.716	0.073	0.062	0.102

Dataset Scaling To investigate the effect of pre-training data scale on performance, we train TimeRCD on increasingly larger subsets of our synthetic dataset: 350M, 700M, and the full 2.5B data points. The results, shown as a weighted average across our benchmark datasets in the Fig. 7, demonstrate a clear and positive scaling law. As the amount of pre-training data increases, the model’s performance consistently improves across all four evaluation metrics.

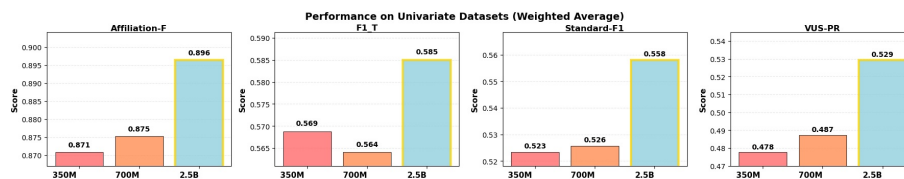


Figure 7: Demonstration of positive scaling laws. The figure shows weighted average performance across our benchmarks when training on datasets of increasing size (350M, 700M, 2.5B).

4 CONCLUSION

In conclusion, TimeRCD successfully addresses the objective mismatch in reconstruction-based methods by introducing the principle of Relative Context Discrepancy. This work establishes a new and effective pre-training paradigm for zero-shot TSAD, with its conceptual simplicity and strong empirical results opening several promising avenues for future research. Looking forward, the extensibility of our framework invites investigation into efficiently fine-tuning the pre-trained TimeRCD on domain-specific datasets for critical applications. As a current limitation and future direction, our implementation relies on a standard transformer backbone; exploring novel network structures specifically engineered to more efficiently capture RCD could yield further performance gains and is a promising area for subsequent research.

ETHICS STATEMENT

In alignment with the ICLR Code of Ethics, this research is committed to upholding the highest standards of academic integrity, social responsibility, and fairness by proactively identifying and mitigating potential ethical risks, ensuring transparency in methodology and limitations, respecting privacy and consent in data usage, promoting inclusivity and non-discrimination, and avoiding any form of harm or misuse, while fostering a constructive and respectful scholarly environment for all participants and the broader community.

REPRODUCIBILITY STATEMENT

We have made every effort to ensure that the results presented in this paper are reproducible. We ensure reproducibility by fully specifying our synthetic data generator (Appx. D). All evaluation datasets and splits follow the TSB-AD protocol described in Appx. E.1. Training configurations—model architecture, optimization, masking strategy, early stopping, and windowing—are detailed in Appx. E.5. Source code is available in <https://anonymous.4open.science/r/TimeRCD-5BE1/>

REFERENCES

- Mohiuddin Ahmed, Abdun Naser Mahmood, and Md Rafiqul Islam. A survey of anomaly detection techniques in financial domain. *Future Generation Computer Systems*, 55:278–288, 2016.
- Abdul Fatir Ansari, Lorenzo Stella, Caner Turkmen, Xiyuan Zhang, Pedro Mercado, Huibin Shen, Oleksandr Shchur, Syama Sundar Rangapuram, Sebastian Pineda Arango, Shubham Kapoor, et al. Chronos: Learning the language of time series. *arXiv preprint arXiv:2403.07815*, 2024.
- Julien Audibert, Pietro Michiardi, Frédéric Guyard, Sébastien Marti, and Maria A Zuluaga. Usad: Un-supervised anomaly detection on multivariate time series. In *Proceedings of the 26th ACM SIGKDD international conference on knowledge discovery & data mining*, pp. 3395–3404, 2020.

- 470 Sathya Kamesh Bhethanabhotla, Omar Swelam, Julien Siems, David Salinas, and Frank Hutter.
471 Mamba4cast: Efficient zero-shot time series forecasting with state space models. *arXiv preprint*
472 *arXiv:2410.09385*, 2024.
- 473
474 Markus M Breunig, Hans-Peter Kriegel, Raymond T Ng, and Jörg Sander. Lof: identifying density-based
475 local outliers. In *Proceedings of the 2000 ACM SIGMOD international conference on Management of*
476 *data*, pp. 93–104, 2000.
- 477 Yifu Cai, Arjun Choudhry, Mononito Goswami, and Artur Dubrawski. Timeseriesexam: A time series
478 understanding exam. *arXiv preprint arXiv:2410.14752*, 2024.
- 479
480 Zahra Zamanzadeh Darban, Yiyuan Yang, Geoffrey I Webb, Charu C Aggarwal, Qingsong Wen, Shirui Pan,
481 and Mahsa Salehi. Dacad: Domain adaptation contrastive learning for anomaly detection in multivariate
482 time series. *IEEE Transactions on Knowledge and Data Engineering*, 2025.
- 483
484 Abhimanyu Das, Weihao Kong, Rajat Sen, and Yichen Zhou. A decoder-only foundation model for time-
485 series forecasting. In *Forty-first International Conference on Machine Learning*, 2024.
- 486
487 Samuel Dooley, Gurnoor Singh Khurana, Chirag Mohapatra, Siddhartha V Naidu, and Colin White. Fore-
488 castpfn: Synthetically-trained zero-shot forecasting. *Advances in Neural Information Processing Systems*,
36:2403–2426, 2023.
- 489
490 Vijay Ekambaram, Subodh Kumar, Arindam Jati, Sumanta Mukherjee, Tomoya Sakai, Pankaj Dayama,
491 Wesley M Gifford, and Jayant Kalagnanam. Tspulse: Dual space tiny pre-trained models for rapid time-
492 series analysis. *arXiv preprint arXiv:2505.13033*, 2025.
- 493
494 Yuchen Fang, Jiandong Xie, Yan Zhao, Lu Chen, Yunjun Gao, and Kai Zheng. Temporal-frequency masked
495 autoencoders for time series anomaly detection. In *2024 IEEE 40th International Conference on Data*
496 *Engineering (ICDE)*, pp. 1228–1241. IEEE, 2024.
- 497
498 Shanghua Gao, Teddy Koker, Owen Queen, Tom Hartvigsen, Theodoros Tsiligkaridis, and Marinka Zitnik.
499 Units: A unified multi-task time series model. *Advances in Neural Information Processing Systems*, 37:
140589–140631, 2024.
- 500
501 Rakshitha Godahewa, Christoph Bergmeir, Geoffrey I Webb, Rob J Hyndman, and Pablo Montero-Manso.
502 Monash time series forecasting archive.
- 503
504 Mononito Goswami, Konrad Szafer, Arjun Choudhry, Yifu Cai, Shuo Li, and Artur Dubrawski. Moment: A
505 family of open time-series foundation models. *arXiv preprint arXiv:2402.03885*, 2024.
- 506
507 Shi Bin Hoo, Samuel Müller, David Salinas, and Frank Hutter. From tables to time: How tabpfn-v2 outper-
508 forms specialized time series forecasting models. *arXiv preprint arXiv:2501.02945*, 2025.
- 509
510 Alexis Huet, Jose Manuel Navarro, and Dario Rossi. Local evaluation of time series anomaly detection
511 algorithms. In *Proceedings of the 28th ACM SIGKDD Conference on Knowledge Discovery and Data*
512 *Mining*, pp. 635–645, 2022.
- 513
514 Deepak A Kaji, John R Zech, Jun S Kim, Samuel K Cho, Neha S Dangayach, Anthony B Costa, and Eric K
515 Oermann. An attention based deep learning model of clinical events in the intensive care unit. *PLoS one*,
14(2):e0211057, 2019.
- 516
517 Tian Lan, Yifei Gao, Yimeng Lu, and Chen Zhang. Cicada: Cross-domain interpretable coding for anomaly
518 detection and adaptation in multivariate time series. *arXiv preprint arXiv:2505.00415*, 2025.

- 517 Fei Tony Liu, Kai Ming Ting, and Zhi-Hua Zhou. Isolation forest. In *2008 eighth ieee international confer-*
518 *ence on data mining*, pp. 413–422. IEEE, 2008.
- 519
- 520 Qinghua Liu and John Paparrizos. The elephant in the room: Towards a reliable time-series anomaly detec-
- 521 *tion benchmark. Advances in Neural Information Processing Systems*, 37:108231–108261, 2024.
- 522
- 523 Youngeun Nam, Susik Yoon, Yooju Shin, Minyoung Bae, Hwanjun Song, Jae-Gil Lee, and Byung Suk Lee.
- 524 Breaking the time-frequency granularity discrepancy in time-series anomaly detection. In *Proceedings of*
525 *the ACM Web Conference 2024*, pp. 4204–4215, 2024.
- 526 Yuqi Nie, Nam H Nguyen, Phanwadee Sinthong, and Jayant Kalagnanam. A time series is worth 64 words:
- 527 Long-term forecasting with transformers. *arXiv preprint arXiv:2211.14730*, 2022.
- 528
- 529 John Paparrizos, Paul Boniol, Themis Palpanas, Ruey S Tsay, Aaron Elmore, and Michael J Franklin. Vol-
- 530 *ume under the surface: a new accuracy evaluation measure for time-series anomaly detection. Proceedings*
531 *of the VLDB Endowment*, 15(11):2774–2787, 2022.
- 532 Hansheng Ren, Bixiong Xu, Yujing Wang, Chao Yi, Congrui Huang, Xiaoyu Kou, Tony Xing, Mao Yang,
- 533 Jie Tong, and Qi Zhang. Time-series anomaly detection service at microsoft. In *Proceedings of the 25th*
534 *ACM SIGKDD international conference on knowledge discovery & data mining*, pp. 3009–3017, 2019.
- 535 M Saquib Sarfraz, Mei-Yen Chen, Lukas Layer, Kunyu Peng, and Marios Koulakis. Position: Quo vadis,
- 536 *unsupervised time series anomaly detection? In International Conference on Machine Learning*, pp.
537 43461–43476. PMLR, 2024.
- 538
- 539 Lifeng Shen, Zhuocong Li, and James Kwok. Timeseries anomaly detection using temporal hierarchical
- 540 *one-class network. Advances in neural information processing systems*, 33:13016–13026, 2020.
- 541
- 542 Qichao Shentu, Beibu Li, Kai Zhao, Yang Shu, Zhongwen Rao, Lujia Pan, Bin Yang, and Chenjuan Guo.
- 543 Towards a general time series anomaly detector with adaptive bottlenecks and dual adversarial decoders.
544 *arXiv preprint arXiv:2405.15273*, 2024.
- 545 Xiaoming Shi, Shiyu Wang, Yuqi Nie, Dianqi Li, Zhou Ye, Qingsong Wen, and Ming Jin. Time-moe:
- 546 Billion-scale time series foundation models with mixture of experts. *arXiv preprint arXiv:2409.16040*,
547 2024.
- 548
- 549 Ya Su, Youjian Zhao, Chenhao Niu, Rong Liu, Wei Sun, and Dan Pei. Robust anomaly detection for
- 550 *multivariate time series through stochastic recurrent neural network. In Proceedings of the 25th ACM*
551 *SIGKDD international conference on knowledge discovery & data mining*, pp. 2828–2837, 2019.
- 552
- 553 Ege Onur Taga, Muhammed Emrullah Ildiz, and Samet Oymak. Timepfn: Effective multivariate time se-
- 554 *ries forecasting with synthetic data. In Proceedings of the AAAI Conference on Artificial Intelligence*,
555 *volume 39*, pp. 20761–20769, 2025.
- 556
- 557 Shreshth Tuli, Giuliano Casale, and Nicholas R Jennings. Tranad: deep transformer networks for anomaly
- 558 *detection in multivariate time series data. Proceedings of the VLDB Endowment*, 15(6):1201–1214, 2022.
- 559
- 560 Ashish Vaswani, Noam Shazeer, Niki Parmar, Jakob Uszkoreit, Llion Jones, Aidan N Gomez, Łukasz Kaiser,
- 561 and Illia Polosukhin. Attention is all you need. *Advances in neural information processing systems*, 30,
562 2017.
- 563
- 564 Garrett Wilson, Janardhan Rao Doppa, and Diane J Cook. Calda: Improving multi-source time series domain
- 565 *adaptation with contrastive adversarial learning. IEEE transactions on pattern analysis and machine*
566 *intelligence*, 45(12):14208–14221, 2023.

564 Lawrence Wong, Dongyu Liu, Laure Berti-Equille, Sarah Alnegheimish, and Kalyan Veeramachaneni. Aer:
565 Auto-encoder with regression for time series anomaly detection. In *2022 IEEE International Conference*
566 *on Big Data (Big Data)*, pp. 1152–1161, 2022. doi: 10.1109/BigData55660.2022.10020857.

567 Gerald Woo, Chenghao Liu, Akshat Kumar, Caiming Xiong, Silvio Savarese, and Doyen Sahoo. Unified
568 training of universal time series forecasting transformers. 2024.

570 Xingjian Wu, Xiangfei Qiu, Zhengyu Li, Yihang Wang, Jilin Hu, Chenjuan Guo, Hui Xiong, and Bin Yang.
571 Catch: Channel-aware multivariate time series anomaly detection via frequency patching. In *The Thir-*
572 *teenth International Conference on Learning Representations*.

573 Shifeng Xie, Vasili Feofanov, Marius Alonso, Ambroise Odonnat, Jianfeng Zhang, Themis Palpanas, and
574 Ievgen Redko. Cauker: classification time series foundation models can be pretrained on synthetic data
575 only. *arXiv preprint arXiv:2508.02879*, 2025.

577 Zhe Xie, Zeyan Li, Xiao He, Longlong Xu, Xidao Wen, Tieying Zhang, Jianjun Chen, Rui Shi, and Dan
578 Pei. Chatts: Aligning time series with llms via synthetic data for enhanced understanding and reasoning.
579 *arXiv preprint arXiv:2412.03104*, 2024.

580 Jiehui Xu, Haixu Wu, Jianmin Wang, and Mingsheng Long. Anomaly transformer: Time series anomaly
581 detection with association discrepancy. *arXiv preprint arXiv:2110.02642*, 2021.

583 Mohammed A Yahya, Antonio R Moya, and Sebastián Ventura. Deep learning for multivariate time series
584 anomaly detection: an evaluation of reconstruction-based methods. *Artificial Intelligence Review*, 58(12):
585 400, 2025.

586 Yiyuan Yang, Chaoli Zhang, Tian Zhou, Qingsong Wen, and Liang Sun. Dcdetector: Dual attention con-
587 trastive representation learning for time series anomaly detection. In *Proceedings of the 29th ACM*
588 *SIGKDD conference on knowledge discovery and data mining*, pp. 3033–3045, 2023.

589 Zahra Zamanzadeh Darban, Geoffrey I Webb, Shirui Pan, Charu Aggarwal, and Mahsa Salehi. Deep learning
590 for time series anomaly detection: A survey. *ACM Computing Surveys*, 57(1):1–42, 2024.

592 Chuxu Zhang, Dongjin Song, Yuncong Chen, Xinyang Feng, Cristian Lumezanu, Wei Cheng, Jingchao Ni,
593 Bo Zong, Haifeng Chen, and Nitesh V Chawla. A deep neural network for unsupervised anomaly detec-
594 tion and diagnosis in multivariate time series data. In *Proceedings of the AAAI conference on artificial*
595 *intelligence*, volume 33, pp. 1409–1416, 2019.

596
597
598
599
600
601
602
603
604
605
606
607
608
609
610